Biomineralization of Sr by the Cyanobacterium *Pseudanabaena catenata* Under Alkaline Conditions

Lynn Foster[1]*, Katherine Morris[1], Adrian Cleary[1], Heath Bagshaw[2], David Sigee[1], Jon K. Pittman[1], Kejing Zhang[1], Gianni Vettese[1], Kurt F. Smith[3] and Jonathan R. Lloyd[1]*

[1] Department of Earth and Environmental Sciences, Research Centre for Radwaste Disposal and Williamson Research Centre for Molecular Environmental Science, The University of Manchester, Manchester, United Kingdom, [2] School of Engineering, University of Liverpool, Liverpool, United Kingdom, [3] Chemical Sciences Division, Lawrence Berkeley National Laboratory, Berkeley, CA, United States

A non-axenic culture of *Pseudanabaena catenata*, a close relative of the bloom-forming cyanobacterium found in the high pH First Generation Magnox Storage Pond at the Sellafield Nuclear Facility, was supplemented with 1 mM of $SrCl_2$, to determine its effect on the fate of Sr. The addition of 1 mM Sr to the *P. catenata* culture resulted in ~16% reduction in the overall growth of the culture (OD_{600nm}) and a 21% reduction in the concentration of chlorophyll-a (Chl-a) compared to those without Sr. The fate of Sr was assessed using a multi-technique approach. Inductively coupled plasma atomic emission spectroscopy showed that virtually all of the Sr was removed from solution, while extracellular biomineral precipitates were analyzed using transmission electron microscopy analysis, and were shown to contain Sr, Ca, and S using energy-dispersive X-ray spectroscopy analysis. In addition, intracellular P-containing electron-dense features, likely to be polyphosphate bodies, were associated with the *P. catenata* cells and contained Sr. Bulk analysis of the cultures by X-ray diffraction showed the presence of Ca-containing strontianite whilst Extended X-ray Absorption Fine Structure analysis showed the presence of strontium phosphate minerals. The presence of Sr associated with intracellular polyphosphate was unexpected, and contrasts with other model photosynthetic systems in the literature that have highlighted carbonate biominerals as the dominant sink for Sr. Understanding the fate of Sr with microorganisms associated with the Spent Nuclear Fuel Ponds (SNFPs) is crucial to understanding the fate of radioactive ^{90}Sr in such extreme environments, and could also suggest a potential remediation strategy for treatment of ^{90}Sr contaminated waters from Spent Nuclear Fuel Ponds SNFPs and in contaminated aquatic systems.

Keywords: first generation magnox storage pond, cyanobacteria, Sr behaviour, transmission electron microscopy, polyphosphate bodies, extended X-ray absorption fine structure

INTRODUCTION

The generation of energy and the development of weapons by the nuclear industry has resulted in the production of significant levels of radioactive material (Wilson, 1996; Crossland, 2012). Despite efforts to contain these radioactive materials, accidental releases have occurred, for example the accidents associated with the nuclear reactors at the Chernobyl (Ukraine) and Fukushima (Japan) sites (Krejci et al., 2011; Fukuda et al., 2014; Chen et al., 2019; Kashparov et al., 2019). The release of radionuclides into the environment requires effective remediation strategies to be employed to

minimize their transport and any harmful effects. There has been a lot of interest in the potential use of microorganisms in cost-effective and efficient remediation strategies, since they are ubiquitous in the environment and have a diverse range of metabolic capabilities (Blanco-Rivero et al., 2005; Pikuta et al., 2007). A wide range of microorganisms, including bacteria, cyanobacteria, eukaryotic algae and fungi are known to influence the speciation and fate of radionuclides by either metabolism-independent or dependent mechanisms (Gadd, 1990).

Of particular interest is the removal of fission products, such as ^{137}Cs and ^{90}Sr from aquatic environments, since they are not only radioactive but also bioavailable, as analogues for K^+ and Ca^{2+}, respectively (Simonoff et al., 2007; Brookshaw et al., 2012; Fukuda et al., 2014). The ability of microorganisms to influence the fate of these high yield and key fission products has been demonstrated, for example with high levels of ^{137}Cs uptake by the eukaryotic microalga species *Coccomyxa actinabiotis* (Rivasseau et al., 2013). The fate of ^{90}Sr appears to be strongly linked to Ca behaviour with, for example, co-association with carbonate minerals that can precipitate out of solution or adsorb to surfaces (Lauchnor et al., 2013; Fukuda et al., 2014; Kang et al., 2014). The majority of carbonate mineral formation is thought to occur as extracellular precipitates that can adsorb to a variety of surfaces including clays and extracellular features of microorganisms (Gadd, 1990; Schultze-Lam and Beveridge, 1994; Chiang et al., 2010). Strontium carbonate formation has recently been shown to occur intracellularly in a small number of microorganisms including the desmid green alga *Closterium moniliferum*, and more recently some cyanobacterial species, e.g., *Gloeomargarita lithophora* (Krejci et al., 2011; Couradeau et al., 2012; Cam et al., 2015; Cam et al.,2016). More recently *G. lithophora* has been shown to be able to effectively remove ^{90}Sr from solution at low concentrations and in the presence of significantly higher concentrations of competing cations and is therefore a good candidate for bioremediation studies (Mehta et al., 2019). In addition Sr is known to interact with phosphate, for example, it can interact with biologically precipitated hydroxyapatite which can be formed by microbial communities supplied with glycerol 2-phosphate (Handley-Sidhu et al., 2014), and a proportion of the intracellular sequestration of stable Sr by *G. lithophora* has been shown to be associate with polyphosphate (Cam et al., 2016). Li et al. (2016) observed that traditional electron microscopy methods used to prepare microbial cells for examination of ultrastructure and sites of metal accumulation, can result in the removal or distortion of such features, and therefore give a false account of intracellular carbonate biomineralization. Indeed, the number of microbial species which are identified as being capable of forming such intracellular carbonate minerals may increase with improvements in preparation techniques.

In the United Kingdom, legacy waste from early Magnox gas-cooled nuclear reactors has been stored in the First Generation Magnox Storage Pond (FGMSP). The FGMSP is an open air spent nuclear fuel pond (SNFP) on the Sellafield nuclear complex (Cumbria, United Kingdom), in operation since the late 1950s (Wilson, 1996; Sellafield, 2014). Magnox reactor fuel consisted of unenriched uranium metal clad in a magnesium non-oxide (MAGNOX) alloy, which both have low chemical stabilities in water (Gregson et al., 2011a; Jackson et al., 2014). The MAGNOX fuel was originally intended for reprocessing, but in some cases has been stored in the FGMSP for considerably longer than anticipated, which has led to extensive corrosion of the MAGNOX cladding and fuel (Jackson et al., 2014). As a result of fuel corrosion, the pond has significant levels of radioactivity including ^{90}Sr and ^{137}Cs associated with the corroded spent nuclear fuel (NDA, 2016), pond effluent, and radioactive sludge (Gregson et al., 2011a, Gregson et al., 2011b; Jackson et al., 2014), of which a major constituent is brucite ($Mg(OH)_2$) (Ashworth et al., 2018). In addition to the radioactive inventory, the pond is open to the air and so it is subject to an influx of carbon, nitrogen and environmental debris (Gregson et al., 2011a, 2011b; Jackson et al., 2014). The pond is continuously purged with alkaline dosed demineralized water at alkaline pH (~11.4), which provides thermal cooling whilst minimizing any further corrosion to the fuel (Gregson et al., 2011a; Gregson et al., 2011b; Jackson et al., 2014; Foster et al., 2020a).

Despite the elevated pH and radionuclide inventory in the FGMSP, microorganisms are known to colonize the pond, with extensive growth periods observed and reported as algal blooms (Foster et al., 2020a; Gregson et al., 2011a; Gregson et al., 2011b). Recently the microbial community of the pond has been investigated using DNA-based tools over a three year period including during a bloom event in August 2016 (Foster et al., 2020a). The pond community of background water samples taken in non-bloom periods was shown to be dominated by *Proteobacteria*, with photosynthetic or hydrogen-metabolizing capabilities present in abundant members of the population (Foster et al., 2020a). During the August 2016 bloom event, the cyanobacterium, *P. catenata* (Foster et al., 2020a) was the most abundant organism detected, making up ~30% of the 16S rRNA genes sequenced in water samples. Despite its presence in a range of other environments and in algal blooms (Acinas et al., 2009; Zhu et al., 2015), there is little information in the scientific literature about the ecology of this filamentous cyanobacterium. Recently the response of a *Pseudanabaena catenata* culture, shown to be a close relative of the cyanobacterium in the pond, to ionizing radiation was documented (Foster et al., 2020b). The culture continued to grow when subjected to a total of 95 Gy over a 5 days period and showed elevated polysaccharide production as a result of the treatment. Currently there is no information on how this organism, which is highly relevant to a radioactive storage facility affects the fate and speciation of key radionuclides and fission products.

The FGMSP is currently undergoing decommissioning as a high priority. This includes planning for waste retrieval operations over 10 years plus timescales and more recently has involved the start of removal of the radioactive sludge inventory (Sellafield, 2014). It is important to understand the potential fate of key radionuclides in the pond during plant operations, to ensure predictable and safe management. While

Sr is present in pond waters at low levels, ^{90}Sr is present at significant levels by activity (average of 160 Bq ml^{-1} during the sampling campaign reported in Foster et al., 2020a) and is potentially very soluble, and thus needs to be considered carefully during effluent processing to minimize discharges to the environment (Ashworth et al., 2018). The purpose of this investigation was to determine the fate of Sr in the presence of microorganisms representative of those in the FGMSP system, namely a mixed laboratory culture dominated by *P. catenata*, a good model for the pond community since it is a close relative to the cyanobacterium identified in the FGMSP (Foster et al., 2020b). This study also aimed to determine whether under the conditions of study, intracellular Sr-containing minerals could be formed by this species of cyanobacterium. Here we demonstrate that in the presence of an actively growing *P. catenata* culture, both strontium carbonate and strontium phosphate biominerals are formed. Interestingly, Sr could be observed by transmission electron microscopy (TEM) and energy-dispersive X-ray spectroscopy (EDS) analysis in association with the electron dense intracellular features containing P, thought to be polyphosphate bodies. Understanding the interactions between Sr and the *P. catenata* culture provides insight into the potential fate of Sr in the pond and may provide pathways toward potential remediation strategies in other ^{90}Sr contaminated aquatic sites.

MATERIALS AND METHODS

Culturing of *Pseudanabaena catenata* With Sr

Experiments were set up to investigate the interaction and fate of Sr with a cyanobacterium, *P. catenata,* which has been identified in the FGMSP on the Sellafield site (Foster et al., 2020a). Radiological control measures in place at the Sellafield site for the FGMSP prevented the isolation and culturing of microorganisms directly from pond water. A photosynthetic culture dominated by *P. catenata*, which is a close match to the species identified in the FGMSP, was obtained from the NIVA Culture Collection of Algae (NIVA-CYA 152), Norway. Whilst it was not possible to source an axenic culture, previous 16S rRNA gene sequencing revealed that of the nine operational taxonomic units identified in the NIVA-CYA 152 culture, five were affiliated with genera identified in the FGMSP (Foster et al., 2020b). The *P. catenata* culture used in the current work was therefore considered representative of the pond community.

Cultures were set up by inoculating the *P. catenata* culture into 30 ml of unbuffered BG11 medium (Culture Collection of Algae and Protozoa) to a starting optical density (600 nm) of 0.2. Three biological replicates were spiked with SrCl$_2$ (Sigma-Aldrich) solution to a final concentration of approximately 1 mM, which is significantly higher than the concentration of active Sr observed in the FGMSP but was used as a compromise between relevance to the system and ability to sensibly analyze the Sr in the experiments. A further three identical cultures were

set up with sterile deionized water used to adjust the total volume in line with the Sr-containing cultures, to assess the impact of Sr on the growth of the culture. All cultures were incubated at 25 ± 1°C, and shaken at 100 rpm in a light incubator with a photon flux density of 150 μmol m^{-2} s^{-1}, with a 16:8 h light-dark cycle (supplied by cool fluorescent daylight lamps). Sterile controls were also set up using 30 ml BG11 medium with 1 mM SrCl$_2$ to determine the effect of abiotic vs. biotic processes.

Optical Density, Chlorophyll-A Concentration, and pH Measurements

In order to determine whether the addition of Sr affected the growth of *P. catenata*, optical density, chlorophyll-a (Chl-a) concentration and pH measurements were taken at selected time points throughout the experiment. All optical density measurements were carried out on 1 ml samples using a Jenway 6700 UV/Vis spectrophotometer (Bibby Scientific Ltd., Staffordshire, United Kingdom). The growth of the *P. catenata* culture was assessed by measuring optical density at 600 nm (OD$_{600nm}$) to indicate the total biomass present in the cultures. The concentration of Chl-a was determined using the same samples as used for the OD$_{600nm}$ measurements, as described in Foster et al. (2020b). Briefly, the cells from a 1 ml sample were pelleted by centrifuging at 14,000g for 10 min and the supernatant was discarded. The cells were re-suspended in 1 ml 70% ethanol and left in the dark at room temperature for 2 h. The samples were centrifuged for a further 10 min at 14,000g, and the absorbance of the supernatant was recorded at 665 nm (Chl-a) and 750 nm (turbidity correction). The concentration of Chl-a was calculated using the formula as set out by Jespersen and Christoffersen (1987). All pH measurements were made using a calibrated FiveEasyPlus pH Meter (Mettler Toledo Ltd., Leicestershire, United Kingdom).

Assessment of Sr Behaviour

The fate of Sr in the presence of the *P. catenata* culture was determined using a range of analytical techniques.

Inductively Coupled Plasma Atomic Emission Spectroscopy

The concentration of soluble Sr in the culture medium was measured by inductively coupled plasma atomic emission spectroscopy (ICP-AES, Perkin-Elmer Optima 5300 dual view) using a matrix-matched serially diluted Specpure multielement plasma standard solution 4 (Alfa Aesar) for calibration. Briefly, a 600 μL sample was centrifuged at 14,000g for 10 min, 500 μL of supernatant was then added to 9.5 ml of 2% nitric acid prior to analysis.

Electron Microscopy

In order to image any Sr minerals formed during the experiment and their potential interactions with *P. catenata* [and other associated microorganisms present in the culture, since a non-axenic culture could not be sourced (Foster et al., 2020b)]

electron microscopy was carried out on non-fixed samples. Samples (1 ml) were taken after 20 days of incubation for analysis by TEM. The samples were washed twice in sterile demineralized water (centrifuged 10 min at 14,000g). For TEM analysis, 2 μL of the washed cell suspension was dropped onto a copper TEM grid with a carbon film (Agar Scientific, Essex, United Kingdom) and allowed to dry at room temperature. The samples were assessed using a FEI Tecnai T20 LaB6 TEM operating at 200 kV equipped with an Oxford XMax EDS detector. The images were captured with Gatan Digital Micrograph whilst the EDS data analysis was performed using Oxford INCA software.

X-Ray Diffraction

An aliquot of culture containing Sr was centrifuged to pellet the cells, the supernatant was discarded, and the cell pellet was spread evenly over a glass slide and allowed to dry. The sample was then analyzed by X-ray diffraction (XRD) to identify any crystalline Sr-containing minerals present. Measurements were carried out on a Bruker D8 Advance diffractometer, equipped with a Göbel Mirror a Lynxeye detector. The X-ray tube had a Cu source, providing Cu K$_{\alpha 1}$ X-rays with a wavelength of 1.540 Å. The sample was scanned from 5 to 70˚2θ, with a step size of 0.01˚ and a count time of 1.5 s per step. The resultant patterns were evaluated using EVA version 4, which compares experimental data to standards from the ICDD (International Center for Diffraction Data) database.

Extended X-ray Absorption Fine Structure

The coordination environment of Sr in the bulk solid phase was analyzed further using X-ray absorption spectroscopy (XAS). Samples were prepared for XAS by removing the solid phase from the culture media after 20 days by vacuum filtration and then diluting with cellulose to form a pellet with approximately 1% Sr loading. Sr K-edge spectra (16115.26 keV) were collected in transmission mode on Beamline B18 at the Diamond Light Source, Harwell, using a liquid nitrogen cooled cryostat. Multiple scans were averaged, calibrated, background subtracted and normalized using ATHENA (Ravel and Newville, 2005). Artemis was then used to fit Extended X-ray Absorption Fine Structure (EXAFS) spectra to determine the average coordination environment of Sr in the solid phase (Ravel and Newville, 2005). Shells were only included in the fit if they made a statistically significant improvement to the model fit as determined by the F-test (Downward et al., 2007).
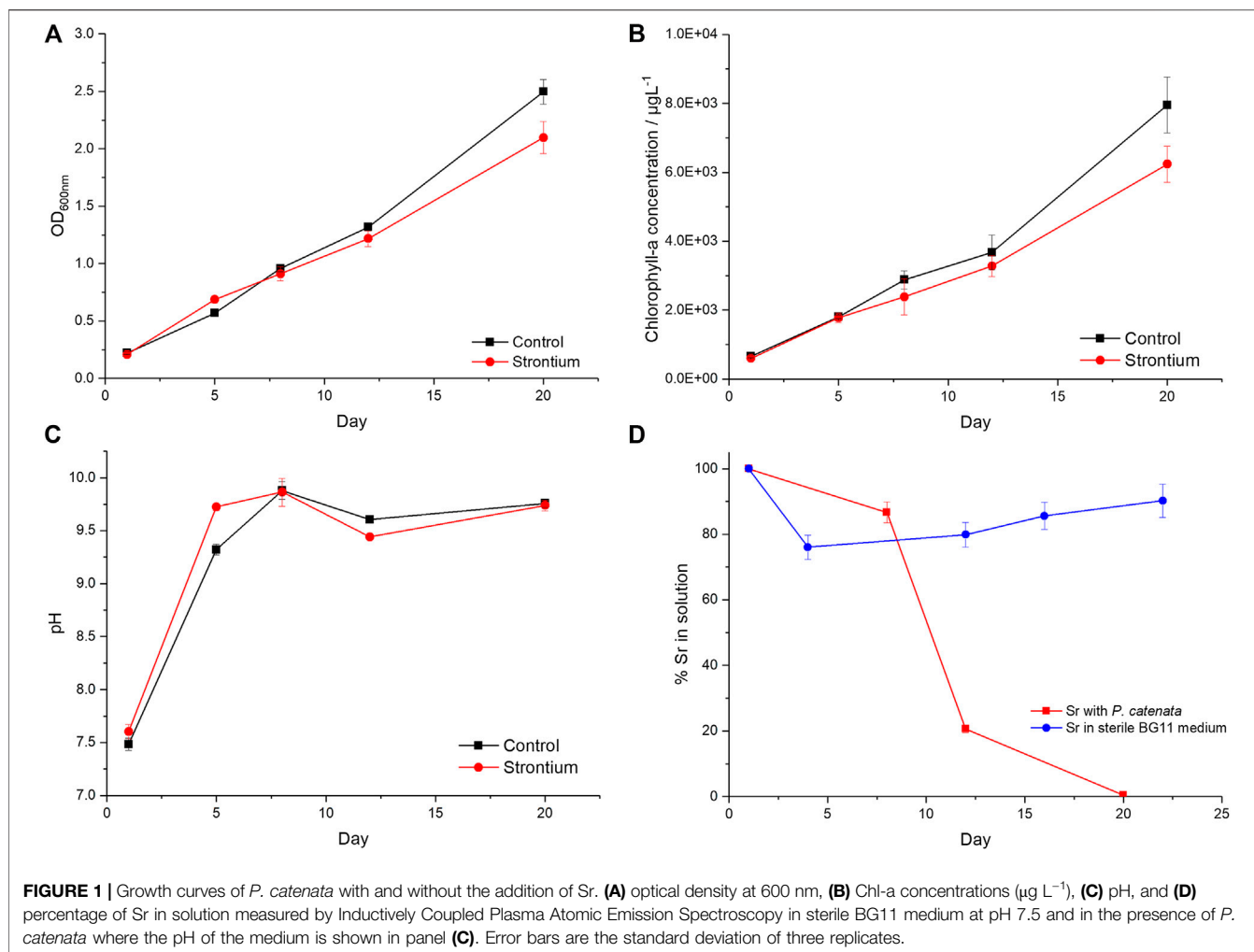
PHREEQC Modeling

All speciation and saturation thermodynamic calculations were performed using the United States Geological Survey thermodynamic speciation code PHREEQC (3.3.7) using the Andra specific interaction theory database (ThermoChimie v.9.b0 August 2015). The modeling was carried out using the concentration of the components of standard BG11 medium (**Supplementary Table 1**) at pH 7.2 and 10.

RESULTS

The Effect of Sr on the Growth of the *P. catenata* Culture

In order to determine whether the addition of Sr had any effect on the growth of the *P. catenata* culture, the optical density and the concentration of Chl-a of the cultures were measured. Measurements were taken over a period of 20 days. When inoculated with an actively growing culture, both the control and Sr-containing cultures showed a steady increase in optical density over the 20-day sampling period as expected (**Figure 1A**). The two sets of treatments started with approximately the same OD$_{600nm}$ measurements of 0.22 [0.01 standard deviation (SD)] for the Sr-free controls compared to 0.21 (0.01 SD) in the Sr-containing cultures. The culture containing Sr grew at the same rate as the control until day 12, indicating that the addition of the Sr did not inhibit growth during the initial phase of growth. The cultures reached their highest optical densities at day 20; 2.49 (0.11 SD) and 2.10 (0.14 SD) for the Sr-free control and Sr-containing cultures respectfully. Assessment of the OD$_{600nm}$ measurements at day 20, using a one-way ANOVA test, shows that there was a significant difference between these measurements (*P*-value 0.01, *F*-ratio 15.3). This indicates that at the end of the sampling period the 1 mM Sr had a subtle but significant inhibitory effect on the final growth yields of the *P. catenata* culture compared to the control. In addition to the OD$_{600nm}$ measurements, the concentration of Chl-a was measured to give an indication of the photosynthetic biomass of the cultures (**Figure 1B**). The cultures started off with Chl-a concentrations of 0.66 mg L^{-1} (0.04 SD) and 0.60 mg L^{-1} (0.04 SD) for the control and Sr-containing cultures, respectively. Both sets of cultures showed a continuous increase in the concentration of Chl-a, which was not significantly different for the first 12 days. At day 20 the concentrations recorded were 7.95 mg L^{-1} (0.82 SD) in the control and 6.23 mg L^{-1} (0.52 SD) in the Sr-containing cultures, which represents a 21% reduction in Chl-a levels between the two treatments. The differences seen between the two treatments at day 20 are significant according to a one-way ANOVA test (*P*-value 0.04, *F*-ratio 9.4). The reduction in the Chl-a concentrations are consistent with the reduction seen in the OD$_{600nm}$ measurements indicating that this is likely to be a consequence of reduced biomass. The pH of the cultures was not controlled by acid or base additions during the course of the experiment, allowing for pH buffering as a result of the photosynthetic activity of *P. catenata*. The pH started at 7.5 (0.1 SD) and 7.6 (0.1 SD) in the control and Sr-containing cultures, respectively (**Figure 1C**). By day 5 the pH of the control cultures had risen to 9.3 (0.01 SD) and the Sr-containing cultures pH 9.7 (<0.01 SD) and these remained elevated over the remaining sampling period. The pH of sterile BG11 medium with Sr remained stable over the same experimental period (data not shown), which confirms that observed increase in the pH is driven by photosynthesis (López-Archilla et al., 2004; Jin et al., 2005).

FIGURE 1 | Growth curves of *P. catenata* with and without the addition of Sr. **(A)** optical density at 600 nm, **(B)** Chl-a concentrations ($\mu g\ L^{-1}$), **(C)** pH, and **(D)** percentage of Sr in solution measured by Inductively Coupled Plasma Atomic Emission Spectroscopy in sterile BG11 medium at pH 7.5 and in the presence of *P. catenata* where the pH of the medium is shown in panel **(C)**. Error bars are the standard deviation of three replicates.

Sr Removal From Solution

ICP-AES was used to determine the amount of Sr in solution throughout the experiment (**Figure 1D**). At day 8, 13.5% Sr was removed from solution with the biomass. In the next 4 days a further 65.3% was removed from solution, and by day 20 >99.5% of the total Sr added had been removed. The largest reduction in soluble Sr concentrations coincided with the maximum pH measurements recorded. In contrast, a maximum of 20% of Sr was insoluble in sterile BG11 medium controls at pH 7.5 (**Figure 1D**). This suggests that approximately 20% of the Sr is removed from solution due to abiotic factors, whilst the majority of Sr is removed as a result of the actions of the microbial culture either directly or indirectly.
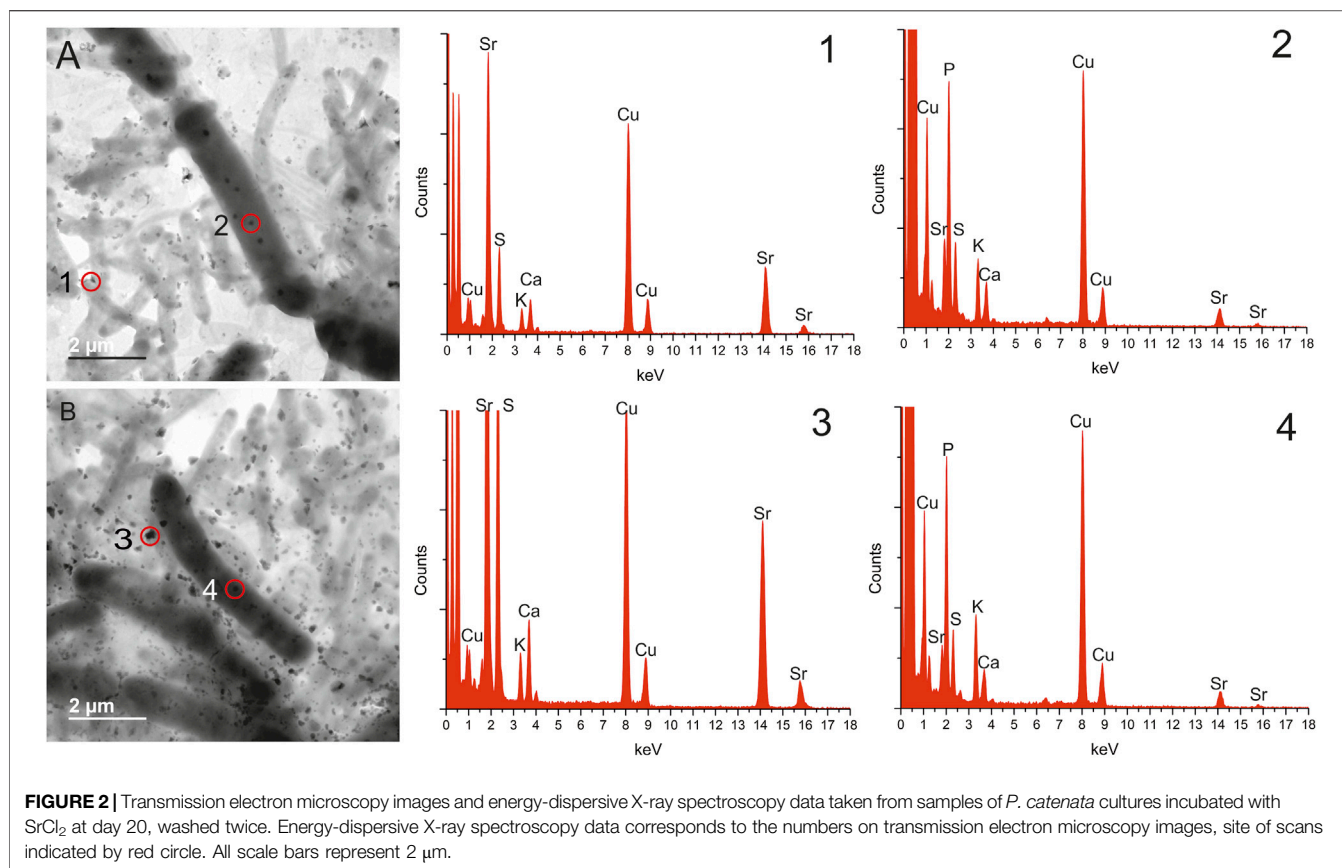
Sr Saturation Calculations

Thermodynamic modeling of 1 mM Sr in BG11 medium (**Supplementary Table 1**) was carried out to identify the products that could precipitate with Sr under representative experimental conditions (**Supplementary Table 2**). The concentration of PO_4^{3-} and CO_3^{2-} in BG11 medium was

0.23 and 0.19 mM, respectively. The modeling indicated when the BG11 medium was at pH 7.2, the strontium phosphate phases $Sr_3(PO_4)_2$ and $Sr_5(PO_4)_3$ were over saturated, suggesting phosphate induced precipitation was possible. When the modeling was repeated at pH 10 (representative of the upper limit of pH in the experiments), the saturation indices [$\log_{10}$ (ion activity/ solubility product)] for the metal phosphate phases increased, indicating that precipitation was more favourable. Here, thermodynamic calculations at the elevated pH (10) suggested that carbonates such as strontianite ($SrCO_3$) were oversaturated.

Determining the Fate of Sr in the *P. catenata* Culture

Electron Microscopy Analysis

TEM was used to analyze samples from the Sr-containing (and control cultures) to assess where the Sr was located and if it was associated with the microorganisms. The samples were washed twice with sterile demineralized water and air dried prior to analysis. Cells were clearly visible in both sets of samples, with

FIGURE 2 | Transmission electron microscopy images and energy-dispersive X-ray spectroscopy data taken from samples of *P. catenata* cultures incubated with SrCl$_2$ at day 20, washed twice. Energy-dispersive X-ray spectroscopy data corresponds to the numbers on transmission electron microscopy images, site of scans indicated by red circle. All scale bars represent 2 μm.
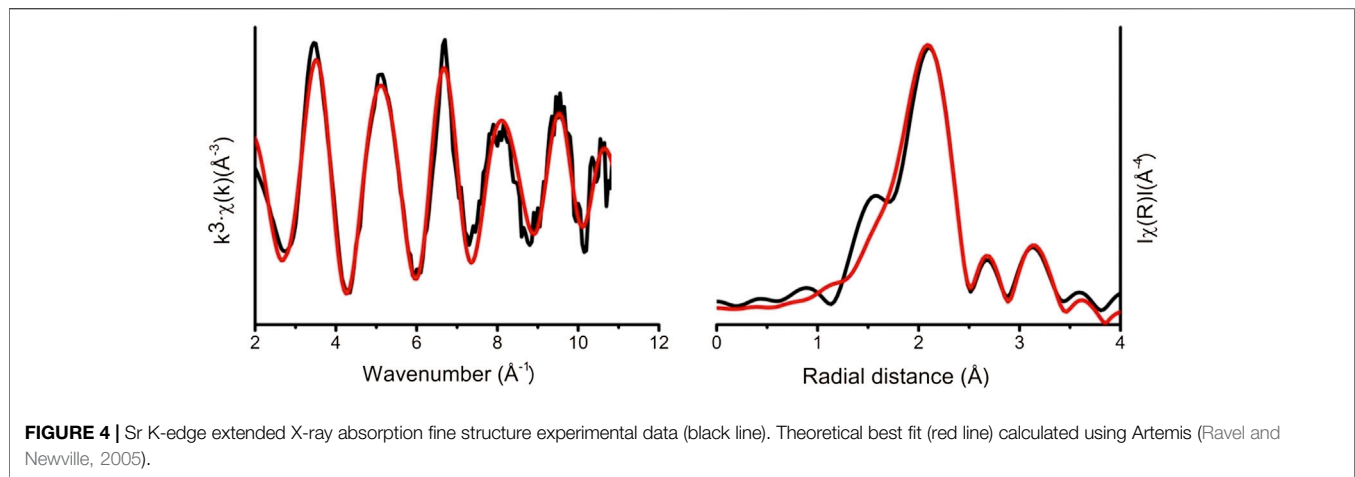
the distinctive *P. catenata* filaments clearly visible (~1 × 5 μm) alongside other smaller heterotrophic microorganisms (Foster et al., 2020b). In both sets of samples *P. catenata* cells displayed circular electron dense features, which frequently occurred in

FIGURE 3 | X-ray diffraction analysis of a bulk sample of *P. catenata* culture incubated with Sr. Red dots indicate the presence of calcian strontianite [(Sr 0.85, Ca 0.15) (CO$_3$)].

the center of and down the length of the filaments (**Figure 2A**; **Supplementary Figure 1**). EDS analysis of these features commonly identified the presence of P, and this suggested that these features could be polyphosphate bodies. In addition, low levels of Ca could also be detected in association with these features. Sr could also be detected with these P-containing structures, indicating that the Sr detected could be intracellular and associated with these structures (**Figure 2**). Significant Sr concentrations could not be detected in other regions of the cells (**Supplementary Figure 2**), offering further support that Sr taken up by the cells was localized with the P-containing features. The micrographs also showed the presence of Sr-containing deposits which appeared to be extracellular but were still associated with the microorganisms (**Figure 2: A1, B3**). EDS analysis of the extracellular deposits showed the presence of Sr, Ca, and S in different proportions but did not show significant P present in these areas.
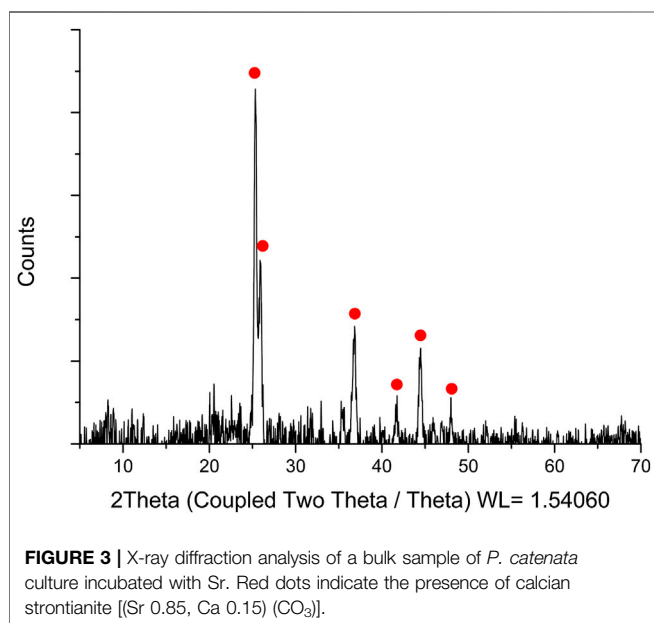
X-Ray Diffraction Characterization of Sr Biominerals

An additional sample of the *P. catenata* precipitate that contained Sr was analyzed using XRD to identify any crystalline minerals that had been formed during the course of the study. The results of the scan indicated the presence of a carbonate mineral, calcian strontianite, which was comprised of Sr and Ca in a ratio of 0.85: 0.15 (**Figure 3**).

FIGURE 4 | Sr K-edge extended X-ray absorption fine structure experimental data (black line). Theoretical best fit (red line) calculated using Artemis (Ravel and Newville, 2005).

Extended X-ray Absorption Fine Structure analysis of Sr Minerals

The average speciation and coordination environment of the Sr in the microbial cultures was further analyzed using XAS. K-edge XANES and EXAFS spectra were collected on Sr in the solid phase. XANES spectra for all samples showed a single peak consistent with a nine-fold coordination environment (Thorpe et al., 2012a; Thorpe et al., 2012b). Modeling of the EXAFS as outer sphere sorbed Sr with a single shell of nine oxygen atoms at a distance of 2.6 Å provided a satisfactory initial fit, however, there were features between 3.2 and 3.6 Å in the Fourier Transform that were not fully resolved with this simple model (**Figure 4**). Further refinement of the EXAFS modeling was informed by the relevant literature on Sr bio-mineral formation (Thorpe et al., 2012b; Bazin et al., 2014; Handley-Sidhu et al., 2014). Here, the best fit was obtained when Sr was coordinated to P with a shell of 1.8 P backscatterers at 3.2 Å and 1 Sr backscattering path at 3.48 Å (**Supplementary Table 3**). These bond lengths are consistent with a strontium phosphate mineral, since the bond lengths of phosphate minerals show high similarity it is not possible to resolve the exact biomineral formed. As XRD data suggested a measurable crystalline fraction of the Sr was present in a crystalline calcian strontianite phase, the EXAFS data were also modeled as $SrCO_3$ and related structures, however this did not yield realistic fits. This suggests the bulk of the Sr is associated with nano-crystalline phosphate mineral phases, consistent with observations from TEM that the polyphosphate-like structures were abundant and also had Ca, Sr, and P co-located.

DISCUSSION

The FGMSP situated on the Sellafield site contains a significant inventory of radioactive fission products, including [90]Sr. This current study investigated the fate of Sr when incubated with a non-axenic culture of *P. catenata*, representative of the microbial community detected in a microbial bloom in the pond in August 2016 (Foster et al., 2020a; Foster et al., 2020b). This is the first study to our knowledge, which investigates the fate of Sr on a mixed microbial community relevant to the microbial ecology of a high pH legacy SNFP.

Collectively our experiments show that the presence of Sr in the culture medium does not substantially prevent the growth of the microorganisms in this mixed culture, although the total biomass at the end of the study period was slightly lower when Sr was present, possibly due to toxicity of the added metal ion. Analysis of the Sr in the culture using EXAFS showed that Sr formed phosphate nanoparticulate phases consistent with thermodynamic modeling predictions suggesting oversaturation of such phases. The TEM data provides evidence that *P. catenata* cells are capable of taking up a small proportion of the Sr in solution, which can become co-localized with polyphosphate type features in the cells. Significant quantities of small extracellular Sr-containing minerals were also visible using the TEM, which varied in their composition, with P not always present. The extracellular minerals appeared to be associated with the outer surfaces of the microorganisms. The extracellular minerals lacking a P peak, are likely to be carbonate minerals, as indicated by XRD analysis. The XRD analysis was not able to confirm the presence of PO_4 minerals in the bulk sample, presumably due to the amorphous character of the nano-particulate strontium phosphate phases observed through EXAFS analyses on the bulk cell precipitates.

Polyphosphate bodies are made up of many orthophosphate residues that are linked by phosphoanhydride bonds to form linear polymers, and can be found in many organisms, and are particularly prevalent in photosynthetic microorganisms (Achbergerová and Nahálka, 2011; Albi and Serrano, 2016; Sanz-Luque et al., 2020). Previous studies have shown that polyphosphate bodies can have a variety of metals associated with them, with the most commonly studied metals including Cd, Pb, and Ca (Baxter and Jensen, 1980; Jensen et al., 1982; Albi and Serrano, 2016). Evidence for Sr interactions with polyphosphate bodies is, however, limited. A study by Baxter and Jensen (Baxter and Jensen, 1980) showed variable uptake of Sr by the cyanobacterium *Plectonema boryanum*. Intracellular Sr, as shown by TEM analysis, was associated with two types of electron dense clusters, the first being polyphosphate bodies whilst the second was devoid of any detectable P. The authors

noted the presence of K in both of the Sr containing electron dense clusters, with the addition of S and Ca features when P was absent. More recently Cam et al. (2016) have shown *G. lithophora* sequestered Sr intracellularly and that a fraction of this was associated with polyphosphate. The authors report the presence of Mg and K associated with the polyphosphate granules (Cam et al., 2016). Interestingly in the current work K, S, and Ca were also observed in the minerals formed in the *P. catenata* culture, including those associated with the polyphosphate type bodies. The Sr containing electron dense bodies seen in the past work with *P. boryanum*, could potentially be carbonate minerals, incorporating both Sr and Ca. Such intracellular Sr carbonates have been the focus of more recent studies using *G. lithophora* and *Cyanothece* sp. PCC7425, where *G. lithophora* showed selective uptake and carbonate mineral formation with Sr (Couradeau et al., 2012; Benzerara et al., 2014; Cam et al., 2015; Cam et al., 2016). The ability to form intracellular carbonate minerals does not appear to be ubiquitous, with *P. catenata* appearing to be incapable of such intracellular mineral formation.

The uptake of small amounts of Sr in *P. catenata,* which are localized at distinct features including polyphosphate, is potentially significant, particularly during microbial bloom periods. There are multiple functions associated with polyphosphate in organisms, including the detoxification of heavy metals (Keasling, 1997; Albi and Serrano, 2016). The level of polyphosphate in microorganisms has been linked to metal tolerance, with higher levels resulting in increased tolerance (Albi and Serrano, 2016) and there is evidence that polyphosphate plays a role in adaptation strategies in extreme environments (Achbergerová and Nahálka, 2011). Further work is required to confirm whether the microorganisms in the FMGSP form polyphosphate bodies and if so what if any metals are associated with them and to see if they show selective sequestration of Sr.

Interactions between the microorganisms in the FGMSP and ^{90}Sr are as yet unknown, however this study provides information about the potential fate of Sr in such systems. In pond effluents ^{90}Sr is present in the water column, suggesting that at least a proportion of the Sr is mobile in the pond. The level of PO_4 in the pond waters has been recorded up to 7.9 mg L^{-1} (Konovalovaite, 2019), whilst Gregson et al. (2011b) reported between 0.3 and 0.8 ppm of P in sampled pond water. The ability of microorganisms to adjust the pH of their surrounding environments and to influence the precipitation and the potential uptake of Sr is of wider interest in contaminated environments, such as the Fukushima site in Japan. Here, it is clear that naturally occurring microbial populations could potentially facilitate a first step in the removal of fission products such as ^{90}Sr from aquatic systems.

DATA AVAILABILITY STATEMENT

All datasets presented in this study are included in the article/ **Supplementary Material**.

AUTHOR CONTRIBUTIONS

LF was the principal author, carried out the experimental work and data analysis. AC collected and analyzed the EXAFS data. HB operated the TEM. DS, JP, and KM developed the concept and reviewed the manuscript. KZ carried out initial experimental trials. KS carried out PHREEQC modeling. JL developed the concept and extensively reviewed the manuscript GV provided analysis of EXAFS data and reviewed the manuscript.

FUNDING

ACKNOWLEDGMENTS

SUPPLEMENTARY MATERIAL

The Supplementary Material for this article can be found online at: https://www.frontiersin.org/articles/10.3389/feart. 2020.556244/full#supplementary-material

REFERENCES

Achbergerová, L., and Nahálka, J. (2011). Polyphosphate—an ancient energy source and active metabolic regulator. *Microb. Cell Fact.* 10, 1–14. doi:10. 1186/1475-2859-10-63

Acinas, S. G., Haverkamp, T. H. A., Huisman, J., and Stal, L. J. (2009). Phenotypic and genetic diversification of *Pseudanabaena* spp. (cyanobacteria). *ISME J.* 3, 31–46. doi:10.1038/ismej.2008.78

Albi, T., and Serrano, A. (2016). Inorganic polyphosphate in the microbial world. Emerging roles for a multifaceted biopolymer. *World J. Microbiol. Biotechnol.* 32, 1–12. doi:10.1007/s11274-015-1983-2

Ashworth, H., Abrahamsen-Mills, L., Bryan, N., Foster, L., Lloyd, J. R., Kellet, S., et al. (2018). Effect of humic acid and bacterial exudates on sorption-desorption interactions of ^{90}Sr with brucite. *Environ. Sci. Process. Impacts* 20, 956–964. doi:10.1039/c8em00073e

Baxter, M., and Jensen, T. (1980). Uptake of magnesium, strontium, barium, and manganese by *Plectonema boryanum* (*Cyanophyceae*) with special reference to polyphosphate bodies. *Protoplasma* 104, 81–89. doi:10.1007/ BF01279371

Bazin, D., Dessombz, A., Nguyen, C., Ea, H. K., Lioté, F., Rehr, J., et al. (2014). Research papers the status of strontium in biological apatites : an XANES/ EXAFS investigation research papers. *J. Synchrotron. Radiat.* 21, 136–142. doi:10.1107/S1600577513023771

Benzerara, K., Skouri-Panet, F., Li, J., Férard, C., Gugger, M., Laurent, T., et al. (2014). Intracellular Ca-carbonate biomineralization is widespread in cyanobacteria. *Proc. Natl. Acad. Sci.* 111, 10933–10938. doi:10.1073/pnas.1403510111

Blanco-Rivero, A., Leganés, F., Fernández-Valiente, E., Calle, P., and Fernández-Piñas, F. (2005). *mrpA*, a gene with roles in resistance to Na$^+$ and adaptation to alkaline pH in the cyanobacterium *Anabaena* sp. PCC7120. *Microbiology* 151, 1671–1682. doi:10.1099/mic.0.27848-0

Brookshaw, D. R., Pattrick, R. A. D., Lloyd, J. R., and Vaughan, D. J. (2012). Microbial effects on mineral-radionuclide interactions and radionuclide solid-phase capture processes. *Mineral. Mag.* 76, 777–806. doi:10.1180/minmag.2012.076.3.25

Cam, N., Georgelin, T., Jaber, M., Lambert, J.-F., and Benzerara, K. (2015). *In vitro* synthesis of amorphous Mg-, Ca-, Sr- and Ba-carbonates: what do we learn about intracellular calcification by cyanobacteria? *Geochim. Cosmochim. Acta* 161, 36–49. doi:10.1016/j.gca.2015.04.003

Cam, N., Benzerara, K., Georgelin, T., Jaber, M., Lambert, J.-F., Poinsot, M., et al. (2016). Selective uptake of alkaline earth metals by cyanobacteria forming intracellular carbonates. *Environ. Sci. Technol.* 50, 11654–11662. doi:10.1021/acs.est.6b02872

Chen, F., Hu, J., Takahashi, Y., Yamada, M., Rahman, M. S., and Yang, G. (2019). Application of synchrotron radiation and other techniques in analysis of radioactive microparticles emitted from the Fukushima Daiichi Nuclear Power Plant accident—a review. *J. Environ. Radioact.* 196, 29–39. doi:10.1016/j.jenvrad.2018.10.013

Chiang, P. N., Wang, M. K., Huang, P. M., Wang, J. J., and Chiu, C. Y. (2010). Cesium and strontium sorption by selected tropical and subtropical soils around nuclear facilities. *J. Environ. Radioact.* 101, 472–481. doi:10.1016/j.jenvrad.2008.10.013

Couradeau, E., Benzerara, K., Gérard, E., Moreira, D., Bernard, S., Brown, G. E., et al. (2012). An early-branching microbialite cyanobacterium forms intracellular carbonates. *Science.* 336, 459–462. doi:10.1126/science.1216171

Crossland, I. (2012). *Nuclear fuel cycle science and engineering.* 1st Edn , Editors I. Crossland (Philadelphia, United States: Woodhead Publishing).

Downward, L., Booth, C. H., Lukens, W. W., and Bridges, F. (2007). A variation of the F-test for determining statistical relevance of particular parameters in EXAFS fits. *AIP Conf. Proc.* 882, 129–131. doi:10.1063/1.2644450

Foster, L., Boothman, C., Ruiz-Lopez, S., Boshoff, G., Jenkinson, P., Sigee, D., et al. (2020a). Microbial bloom formation in a high pH spent nuclear fuel pond. *Sci. Total Environ.* 720, 137515. doi:10.1016/j.scitotenv.2020.137515

Foster, L., Muhamadali, H., Boothman, C., Sigee, D., Pittman, J. K., Goodacre, R., et al. (2020b). Radiation tolerance of *Pseudanabaena catenata*, a cyanobacterium relevant to the first generation Magnox storage pond. *Front. Microbiol. Provisiona* 11, 1–13. doi:10.3389/fmicb.2020.00515

Fukuda, S.-y., Iwamoto, K., Atsumi, M., Yokoyama, A., Nakayama, T., Ishida, K.-i., et al. (2014). Global searches for microalgae and aquatic plants that can eliminate radioactive cesium, iodine and strontium from the radio-polluted aquatic environment: a bioremediation strategy. *J. Plant Res.* 127, 79–89. doi:10.1007/s10265-013-0596-9

Gadd, G. M. (1990). Heavy metal accumulation by bacteria and other microorganisms. *Experientia* 46, 834–840. doi:10.1007/BF01935534

Gregson, C. R., Goddard, D. T., Sarsfield, M. J., and Taylor, R. J. (2011a). Combined electron microscopy and vibrational spectroscopy study of corroded Magnox sludge from a legacy spent nuclear fuel storage pond. *J. Nucl. Mater.* 412, 145–156. doi:10.1016/j.jnucmat.2011.02.046

Gregson, C. R., Hastings, J. J., Sims, H. E., Steele, H. M., and Taylor, R. J. (2011b). Characterisation of plutonium species in alkaline liquors sampled from a UK legacy nuclear fuel storage pond. *Anal. Methods* 3, 1957. doi:10.1039/c1ay05313b

Handley-Sidhu, S., Hriljac, J. A., Cuthbert, M. O., Renshaw, J. C., Pattrick, R. A. D., Charnock, J. M., et al. (2014). Bacterially produced calcium phosphate nanobiominerals: sorption capacity, site preferences, and stability of captured radionuclides. *Environ. Sci. Technol.* 48, 6891–6898. doi:10.1021/es500734n

Jackson, S. F., Monk, S. D., and Riaz, Z. (2014). An investigation towards real time dose rate monitoring, and fuel rod detection in a First Generation Magnox Storage Pond (FGMSP). *Appl. Radiat. Isot.* 94, 254–259. doi:10.1016/j.apradiso.2014.08.019

Jensen, T. E., Baxter, M., Rachlin, J. W., and Jani, V. (1982). Uptake of heavy metals by *Plectonema boryanum* (Cyanophyceae) into cellular components, especially polyphosphate bodies: an X-ray energy dispersive study. *Environ. Pollut.* 27, 119–127. doi:10.1016/0143-1471(82)90104-0

Jespersen, A.-M., and Christoffersen, K. (1987). Measurements of chlorophyll-a from phytoplankton using ethanol as extraction solvent. *Arch. Hydrobiol.* 109, 445–454. 0003-9136/87/0109-0445 (ISSM 0003-9136). https://pascal-francis.inist.fr/vibad/index.php?action=getRecordDetail&idt=7612451

Jin, X., Chu, Z., Yi, W., and Hu, X. (2005). Influence of phosphorus on *Microcystis* growth and the changes of other environmental factors. *J. Environ. Sci.* 17, 937–941. 1001-0742(2005) 06-0937-05

Kang, C.-H., Choi, J.-H., Noh, J., Kwak, D. Y., Han, S.-H., and So, J.-S. (2014). Microbially induced calcite precipitation-based sequestration of strontium by *Sporosarcina pasteurii* WJ-2. *Appl. Biochem. Biotechnol.* 174, 2482–2491. doi:10.1007/s12010-014-1196-4

Kashparov, V., Salbu, B., Levchuk, S., Protsak, V., Maloshtan, I., Simonucci, C., et al. (2019). Environmental behaviour of radioactive particles from chernobyl. *J. Environ. Radioact.* 208–209. doi:10.1016/j.jenvrad.2019.106025

Keasling, J. D. (1997). Regulation of intracellular toxic metals and other cations by hydrolysis of polyphosphate. *Ann. N. Y. Acad. Sci.* 829, 242–249. doi:10.1111/j.1749-6632.1997.tb48579.x

Konovalovaite, J. (2019). Control of algae in fuel storage ponds. Ph.D. thesis. Manchester, UK: University of Manchester.

Krejci, M. R., Finney, L., Vogt, S., and Joester, D. (2011). Selective sequestration of strontium in desmid green algae by biogenic co-precipitation with barite. *ChemSusChem* 4, 470–473. doi:10.1002/cssc.201000448

Lauchnor, E. G., Schultz, L. N., Bugni, S., Mitchell, A. C., Cunningham, A. B., and Gerlach, R. (2013). Bacterially induced calcium carbonate precipitation and strontium coprecipitation in a porous media flow system. *Environ. Sci. Technol.* 47, 1557–1564. doi:10.1021/es304240y

Li, J., Margaret Oliver, I., Cam, N., Boudier, T., Blondeau, M., Leroy, E., et al. (2016). Biomineralization patterns of intracellular carbonatogenesis in cyanobacteria: molecular hypotheses. *Minerals* 6, 10. doi:10.3390/min6010010

López-Archilla, A. I., Moreira, D., López-García, P., and Guerrero, C. (2004). Phytoplankton diversity and cyanobacterial dominance in a hypereutrophic shallow lake with biologically produced alkaline pH. *Extremophiles* 8, 109–115. doi:10.1007/s00792-003-0369-9

Mehta, N., Benzerara, K., Kocar, B. D., and Chapon, V. (2019). Sequestration of radionuclides radium-226 and strontium-90 by cyanobacteria forming intracellular calcium carbonates. *Environ. Sci. Technol.* 53, 12639–12647. doi:10.1021/acs.est.9b03982

NDA (2016). Nuclear decommissioning authority: business plan 2017 to 2020. Gov.uk. Available at: https://www.gov.uk/government/consultations/nuclear-decommissioning-authority-business-plan-2017-to-2020 (Accessed May 4, 2018).

Pikuta, E. V., Hoover, R. B., and Tang, J. (2007). Microbial extremophiles at the limits of life. *Crit. Rev. Microbiol.* 33, 183–209. doi:10.1080/10408410701451948

Ravel, B., and Newville, M. (2005). ATHENA, ARTEMIS, HEPHAESTUS: data analysis for X-ray absorption spectroscopy using IFEFFIT. *J. Synchrotron Radiat.* 12, 537–541. doi:10.1107/S0909049505012719

Rivasseau, C., Farhi, E., Atteia, A., Couté, A., Gromova, M., de Gouvion Saint Cyr, D., et al. (2013). An extremely radioresistant green eukaryote for radionuclide bio-decontamination in the nuclear industry. *Energy Environ. Sci.* 6, 1230–1239. doi:10.1039/C2ee23129h

Sanz-Luque, E., Bhaya, D., and Grossman, A. R. (2020). Polyphosphate: a multifunctional metabolite in cyanobacteria and algae. *Front. Plant Sci.* 11, 1–21. doi:10.3389/fpls.2020.00938

Schultze-Lam, S., and Beveridge, T. J. (1994). Nucleation of celestite and strontianite on a cyanobacterial S-layer. *Appl. Environ. Microbiol.* 60, 447–453. doi:10.1128/aem.60.2.447-453.1994

Sellafield (2014). *Sellafield magazine.* 20–29. Available at:https://www.gov.uk/government/publications/sellafield-magazine-issue-4 (Accessed May 30, 2018).

Simonoff, M., Sergeant, C., Poulain, S., and Pravikoff, M. S. (2007). Microorganisms and migration of radionuclides in environment. *Comput. Rendus Chem.* 10, 1092–1107. doi:10.1016/j.crci.2007.02.010

Thorpe, C. L., Lloyd, J. R., Law, G. T. W., Burke, I. T., Shaw, S., Bryan, N. D., et al. (2012a). Strontium sorption and precipitation behaviour during bioreduction

in nitrate impacted sediments. *Chem. Geol.* 306–307, 114–122. doi:10.1016/j. chemgeo.2012.03.001

Thorpe, C. L., Morris, K., Boothman, C., and Lloyd, J. R. (2012b). Alkaline Fe(III) reduction by a novel alkali-tolerant *Serratia* sp. isolated from surface sediments close to Sellafield nuclear facility, UK. *FEMS Microbiol. Lett.* 327, 87–92. doi:10. 1111/j.1574-6968.2011.02455.x

Wilson, P. D. (1996). *The nuclear fuel cycle from ore to waste*. Editor P. D. Wilson (Oxford, England: Oxford University Press).

Zhu, M., Yu, G., Song, G., Chang, J., Wan, C., and Li, R. (2015). Molecular specificity and detection for *Pseudanabaena* (cyanobacteria) species based on *rbcLX* sequences. *Biochem. Syst. Ecol.* 60, 110–115. doi:10.1016/j.bse.2015.04.009